Potential *In Situ* Preparation of Aliphatic Polyamide-Based Nanocomposites: The Organoclay-Polyamide Salt Interaction

A. C. Boussia, Ch. C. Damianou, S. N. Vouyiouka, C. D. Papaspyrides

Laboratory of Polymer Technology, School of Chemical Engineering, National Technical University of Athens, Athens, Greece

Received 28 April 2009; accepted 12 November 2009
DOI 10.1002/app.31753
Published online 22 February 2010 in Wiley InterScience (www.interscience.wiley.com).

ABSTRACT: *In situ* intercalative polycondensation is applied for the preparation of polyamide (PA) *n*,6–clay nanocomposites, namely poly(ethylene adipamide) (PA 2,6), poly(hexamethylene adipamide) (PA 6,6), and poly (dodecamethylene adipamide) (PA 12,6). For this purpose, two different polymerization routes are considered; a low-temperature melt polymerization technique and the conventional solution-melt one. Under the specific experimental conditions, lack of clay exfoliation is detected through XRD measurements, which is proved irreversible even when twin-screw extrusion is attempted as an additional step. The resulting PA *n*,6–clay structures are found dependent on the diamine moiety length; more specifically, an intrinsic interaction between the polyamide monomer and the organoclay surfactant is indicated. An ion exchange occurs between the two competitive species, that is, diamine and surfactant cations, leading to flocculated clay structures. © 2010 Wiley Periodicals, Inc. J Appl Polym Sci 116: 3291–3302, 2010

Key words: nanocomposites; polyamides; organoclay; surfactants

INTRODUCTION

Polymer-layered silicate nanocomposites are a class of materials that has attracted the interest of the academical and lately the industrial world, owing to their exceptional properties. Clay minerals, which play the role of the filler in this composites family, are layered aluminosilicates consisting of stacks of negatively charged two-dimensional sheets. Optimal properties for the nanocomposites, such as mechanical, thermal, barrier, and flame retardant, are obtained when the sheets are randomly dispersed in the polymer matrix so as to gain a large contact area with the matrix.[1,2] To achieve the aforementioned dispersion, pristine clays containing inorganic cations, such as Na^+, K^+, and Ca^{2+}, need to be compatibilized with polymer matrices. Clays become organophilic through an ion exchange reaction between the alkali and an organic surfactant cation, most commonly primary, secondary, tertiary, or quaternary alkylammoniums.[1–4] The surfactant type defines the interlayer spacing: quaternary ammonium salts enlarge more the silicate spacing than primary, while aromatic content further increases it. Additional parameters governing the dispersion of the sheets within the polymer are the type of silicate and its swelling potential associated with the cation exchange capacity (CEC, meq/100 g), energetic/thermodynamic factors associated with the layer structure, the method and the processing conditions, the type of matrix, as well as its molecular weight.[1,2,5–9]

Focusing on poly(hexamethylene adipamide) (PA 6,6), one of the most widely used linear polyamides, several studies have been reported on the formation of PA 6,6–organoclay nanocomposites via melt blending.[1,9–13] The high temperature profiles often result in decomposition of nanofiller surfactant, due to Hofmann elimination reaction, which evolves chemical species such as α-olefins and amines prone to catalyzing degradation of the polymer.[14,15] An alternative method for the production of PA 6,6–clay nanocomposites is *in situ* intercalative polyamidation, which constitutes in polymerizing the monomers diamine–diacid or their derived salt in the presence of the nanofiller, and yields—by definition of the method—nanocomposites characterized by a finer dispersion of the nanofiller, resulting in advanced materials properties. The relevant technique has been extensively and successfully applied on polyamides of aminoacid or lactam starting monomers, such as polycaproamide (PA 6).[1,16] Dissimilarly, the application of *in situ* intercalative polyamidation when starting monomers are either

Correspondence to: C. D. Papaspyrides (kp@softlab.ece.ntua.gr).

diamine–diacid equimolecular solution or their dry salt is rare in published literature.[1,17–20]

Based on the limited literature on *in situ* intercalative polyamidation, the achievement of exfoliated structures seems to be case sensitive, depending on the nature of matrix,[18] polymerization conditions,[18] montmorillonite type, as well as the surfactant used.[17,18] Indeed, Goettler and Joardar[18] reported the formation of PA 6,6–clay nanocomposites via *in situ* solution-melt (SM) polycondensation, highlighting the dependence of fully exfoliated structure on the absence of ionic exposure during polymerization. The latter would be ideally achieved—as therein proposed—by inserting the organoclay in the melt state of the polymerization following water removal. Song et al.[17] similarly formed exfoliated PA 6,6–clay nanocomposites through melt polycondensation of the relevant diamine–diacid salt, via modifying first the pristine clay with aminocaproic acid. Apart from a suitable surfactant, the use of a low CEC clay was preferred, to avoid inhibition of the surfactant spatial arrangement because of its high concentration, on the intercalation of growing polymer. Nevertheless, in some cases, flocculated structures were derived, which were attributed to thermal degradation of the organoclay surfactant and to the subsequent irreversible diminishment of the clay interlayer spacing. Finally, Wu et al.[19] reported on the formation of exfoliated poly(decamethylene dodecanamide) (PA 10,12)–organoclay nanocomposite by melt polycondensation of the relevant PA salt, although the obtained XRD spectrum might evidence partial aggregation of clay sheets, based on a residual peak corresponding to interlayer spacing shorter than the initial one.

This article is oriented in the synthesis of PA *n*,6–clay nanocomposites via *in situ* polycondensation. The effect of the polyamide type (PA *n*,6) on clay dispersion is investigated, in parallel with the type of clay (pristine or variably organomodified). The polyamidation is initially carried out in a small scale, with the application of a low-temperature melt (LTM) polycondensation technique, which has been patented in the past by Papaspyrides et al. in cooperation with DuPont, Delaware.[21–23] The relevant process proceeds in the absence of solvents using as starting material dry PA salt and operates in the vicinity of the melting point of the salt. This technique comprises two stages, proceeding first under autogenous pressure conditions to compensate and reduce the loss of volatile diamine from the reaction composition. The second stage comprises venting under constant nitrogen flow, so as to continuously evacuate the reactor from water vapor.[22] Therefore, this technique ensures polyamide grades of sufficient molecular weight and end group balance. Especially, for the case of polyamide nanocomposites, this technique may bear the advantage of avoiding any side effects derived from elevated polymerization temperatures, such as thermal degradation of polyamide matrix, and mainly decomposition of organoclay surfactants. Moreover, the case of PA 6,6–clay nanocomposite is scaled up and the application of the conventional SM polycondensation process is further studied in combination with a final extrusion step (SME).[24] In both polyamidation routes applied, the potential for clay dispersion is investigated, associated with the different polymerization conditions and ultimately with the inherent structure of polyamide monomers.

EXPERIMENTAL

Materials

Diamines of variant aliphatic content were used, namely ethylenediamine (ETD), hexamethylenediamine (HMD), and dodecamethylenediamine (DMD). Adipic acid (AA) and ethanol were used and the reagents were all of analytical grade (Merck, Germany). Cloisite® Na, an unmodified montmorillonite with a CEC of 92.6 meq/100 g, was supplied by Southern Clay Products (Gonzales, USA) and is denoted as MT. Nanofil® 848 and Nanofil® 9 are organoclays based on natural montmorillonite of 95.0 meq/100 g CEC, modified with octadecylammonium chloride (25% w/w) and octadecylbenzyldimethylammonium chloride (30% w/w), respectively, and were provided by Süd Chemie AG (Moosburg, Germany). Nanofil® 848 is herein denoted as OMT1 and Nanofil® 9 as OMT2. All nanofiller concentrations reported hereafter are calculated with respect to inorganic content.

Polyamide monomers

The preparation of polyamide salts involved combining the diamines with adipic acid in exactly molecular proportions, by bringing together ethanol solutions of equivalent amounts of the reactants [eq. (1), $n = 2, 6, 12$][24–32]:

$$\mathrm{HOOC-(CH_2)_4-COOH + H_2N-(CH_2)_n-NH_2} \longrightarrow {}^{-}\mathrm{OOC-(CH_2)_4-COO^{-}\cdot{}^{+}H_3N-(CH_2)_n-NH_3^{+}}. \quad (1)$$

The formed salts precipitated, were filtered, thoroughly washed, and the sediments were dried for 4 h at 50°C *in vacuo*. The salts were then dry blended with nanofillers (2.5% w/w) to form homogeneous mixtures. Especially, for the case of PA 6,6 salt, a hybrid organoclay-containing monomer was additionally prepared, based on previous works by Papaspyrides and Kampouris[26,27] on catalyst

incorporation in PA monomers through coprecipitation. In particular, OMT1 (2.5% w/w) was dispersed either in HMD or AA solution, followed by the addition of AA or HMD solution, respectively. Accordingly, we prepared the following monomer grades: 6,6–MT, *n*,6–OMT1 (n = 2, 6, and 12), 6,6–OMT2, 6,6–OMT1/CP salts, while CP denotes the coprecipitation procedure.

PA *n*,6 nanocomposites via low-temperature melt polycondensation process

An anhydrous low-temperature process was applied to polymerize the salt grades prepared.[21,22] Each monomer grade was loaded in a glass tube, which was fitted in a stainless steel laboratory reactor (50 mL capacity, Parr Instrument), ensuring the absence of oxygen by purging the reactor with inert gas. The polymerization was performed at 200°C in a two-stage process, first under autogenous pressure conditions for 1 h ($P_{max} \approx 5$ bar) and in sequence under N_2 flow (500 mL min^{-1}) for 15 min, maintaining the temperature in the range of 200–225°C. The produced grades were extracted from the reactor as colorless solids (Table I).

PA 6,6 nanocomposites via solution-melt polycondensation process and subsequent extrusion

A solution-melt polymerization process was further applied for the preparation of PA 6,6-based nanocomposite grades, in a stainless steel large-scale laboratory reactor (2 L capacity, Snap Tite). The first stage comprised heating and stirring an aqueous solution (50% w/v) of the monomer grade (T = 225°C, t = 90 min, $P_{max} \approx 30$ bar, ω = 450 rpm), whereas the second stage consisted of venting the reactor, in parallel with N_2 flow (500 mL min^{-1}) and maintenance of the temperature in the range of 225–240°C for 40 min. The produced grades (Table I) were extracted from the reactor as colorless solids (designated as SM), subsequently extruded in a twin-screw corotating intermeshing extruder (designated as SME) (Thermo Fisher Scientific, T = 255–290°C, ω = 150 rpm, *in vacuo*) and pelletized.

Heat treatment of organoclays

The organoclays were subjected for comparison reasons to thermal treatment at the same T–t profiles applied in the described polymerization processes, in which each organoclay was involved. Accordingly, OMT1 and OMT2 (5 g) were heat treated at the T–t profile of LTM polycondensation, while OMT1 was additionally heat treated at the T–t profile of SM one. The derived organoclays are designated as HT_OMT1(LTM), HT_OMT2(LTM), and HT_OMT1(SM).

TABLE I
Monomers and Respective Polyamide–Clay Grades

Monomer grade (2.5% w/w)	Polymer grade (2.5% w/w)
Low-temperature melt polycondensation (LTM)	
2,6–OMT1	PA 2,6–OMT1 (LTM)
6,6–MT	PA 6,6–MT (LTM)
6,6–OMT1	PA 6,6–OMT1 (LTM)
6,6–OMT1/CP	PA 6,6–OMT1/CP (LTM)
6,6–OMT2	PA 6,6–OMT2 (LTM)
12,6–OMT1	PA 12,6–OMT1 (LTM)
Solution-melt polycondensation (SM) and subsequent extrusion (SME)	
6,6–OMT1	PA 6,6–OMT1 (SM) and (SME)
6,6–OMT1/CP	PA 6,6–OMT1/CP (SM) and (SME)

Treatment of organoclay with diamines aqueous solutions

To investigate any ion exchange interaction, as discussed later, OMT1 was dispersed in ETD, HMD, and DMD aqueous solutions. In all dispersions, the amine cation concentration was in excess over the organoclay, equivalent to 25 times the CEC of the inorganic material. The dispersions were vigorously stirred for 1 h. The sediments were filtered, thoroughly dried *in vacuo* and ground, and are designated as OMT1–ETD_{aq}, OMT1–HMD_{aq}, and OMT1–DMD_{aq}.

Characterization

Fourier transform infrared spectroscopy

Infrared spectra were recorded using a Biorad Excalibur FTS 3000MX spectrometer at frequencies from 4000–400 cm^{-1} with a resolution of 4 cm^{-1}. The spectra were obtained from pastilles of the polyamide spread onto KBr crystals.

Solution viscometry

Intrinsic viscosity of synthesized polyamides [η] was measured in *m*-cresol at a concentration of 0.5 g dL^{-1} in an Ubbelohde viscometer at 25°C. The [η] value was obtained by the single-point measurement equation proposed by Solomon and Ciuta[33]:

$$[\eta] = \frac{1}{C}\sqrt{2(\eta_{sp} - \ln\ \eta_{rel})}, \quad (2)$$

where C is the solution concentration (g dL^{-1}), η_{sp} the solution specific viscosity, η_{rel} the solution

relative viscosity. The deviation of the mean values was derived through duplicate measurements.

Differential scanning calorimetry

Thermal properties of synthesized polyamides were determined by DSC measurements in a Perkin Elmer DSC4 from 30 to 300°C with a heating rate of 20°C min^{-1} under nitrogen flow. Crystallinity (X_c) % was calculated from the endothermic curves according to eq. (3):

$$X_c = \frac{\Delta H_m}{\Delta H_0}\%, \quad (3)$$

where ΔH_m (cal g^{-1}) represents the actual heat of melting and ΔH_o is a reference value corresponding to the heat of melting for 100% crystalline polymer, taken as 50.45 cal g^{-1}.[34]

Wide angle X-ray diffraction

All grades were characterized by means of X-ray diffraction. WAXD spectra were collected from a Siemens powder D-5000 Diffractometer equipped with a Cu Ka_1 radiation (λ = 1.5405 Å), operating at 40 kV, 30 mA. The diffraction analysis was performed in the range of 2°–30° (2Θ) for polyamide crystals characterization and 2°–10° for clay dispersion investigation.

RESULTS AND DISCUSSION

PA *n*,6 nanocomposites via low-temperature melt polycondensation process

In the following section, the synthesis of PA *n*,6–clay nanocomposites was assessed by a low-temperature melt polycondensation process in a small scale to investigate the influence of nanofiller type and polyamide repeating unit on clay dispersion. At first, the synthesized polyamides formation was verified qualitatively and quantitatively. The FTIR spectra [Fig. 1(a)] indicated the presence of amide bonds in all PA *n*,6–nanocomposite cases: all grades gave absorptions at 3300 cm^{-1} (amide I, hydrogen-bonded NH vibration) and 1640 (amide I, C=O stretch).[24] Moreover, based on the obtained WAXD profiles [Fig. 1(b)], typical polyamide structures were observed for all different matrices. More specifically, a triclinic lattice (α-form) with the chains in fully extended zigzag conformation was verified for PA 6,6- and PA 12,6-based grades, exhibiting two diffraction peaks at 2Θ ≈ 20.3° (d ≈ 4.4 Å) and 2Θ ≈ 24.0° (d ≈ 3.7 Å) indicative of such structure.[35] Meanwhile, PA 2,6–OMT1(LTM) XRD spectrum indicated a mixture of α-form and *b*-form, as the diffraction peaks were displaced at 2Θ = 21.7° (d = 4.1 Å) and 2Θ = 22.8° (d = 3.9 Å), tending to converge to a single one.[35]

Regarding the thermal properties of synthesized PA *n*,6–clay grades, the melting points were found to decrease with diamine methylene content increase (Table II), while the highest melting point (T_m= 324.21°C) was observed for PA 2,6–OMT1, owing to the high density of amide bonds and thus hydrogen bonding network. For the same reason, PA 2,6–OMT1 presented the highest crystallinity (X_c % = 48.4), while PA 6,6 and PA 12,6 matrices were characterized by decreasing values due to the higher aliphatic content.[36] The intrinsic viscosity values ranged from 0.50 to 0.62 dL g^{-1} (Table II), indicating the formation of low-molecular-weight polyamides in all different matrices, corresponding in the case of PA 6,6 grades to $\overline{M}_v$ varying from 6300 to 8000 g mol^{-1}. These values are satisfactory considering the short reaction time and low reaction temperatures applied[22] and suitable to study the influence of nanofiller type and polyamide repeating unit on clay dispersion, as is the goal of this study. The highest intrinsic viscosity ([η] = 0.62 dL g^{-1}) was observed in the case of PA 12,6 matrix due to lowest volatility of the diamine component, and thus less disturbance of the reaction stoichiometry. Finally, the clay content was determined by ashing to be 2.36% w/w for PA 2,6–OMT1, 2.62% w/w for PA 6,6–OMT1, and 2.42% w/w for PA 12,6–OMT1, being close to the theoretical concentration of 2.5% w/w and confirming the efficient nanofiller incorporation in the polyamide matrices.

Focusing on the influence of nanofiller type (pristine, OMT1, OMT2) on clay dispersion, a structural analysis of the formed polyamide salts through XRD was initially performed before polymerization. The spectra obtained revealed that in the PA 6,6–organoclay coprecipitate salt, the contained silicate was structurally modified, as evidenced by a shift of the nanofiller initial diffraction peak (denoted as d_{001}) from 2Θ = 5.0° to 2Θ= 6.6°, that is, to higher angle than the original one of OMT1 (Fig. 2). More specifically, the relevant angles increase corresponds to a significant decrease of silicate interlayer spacing, from 18.2 to 13.6 Å, occurring during coprecipitation, independently of OMT1 dispersion medium (HMD or AA ethanol solution). On the contrary, in the dry blend case, no silicate sheet collapse occurred, as anticipated.

Turning to the polymerized grades based on PA 6,6 matrix, it can be readily seen in Figure 3 that, despite the different kind of clay used in each grade and the use of dry blend or coprecipitate starting material, silicate sheets failed to completely exfoliate in the polyamide matrix. Interestingly, the *in situ* polymerized grades yielded XRD spectra, characterized by an identical feature: the achievement of the

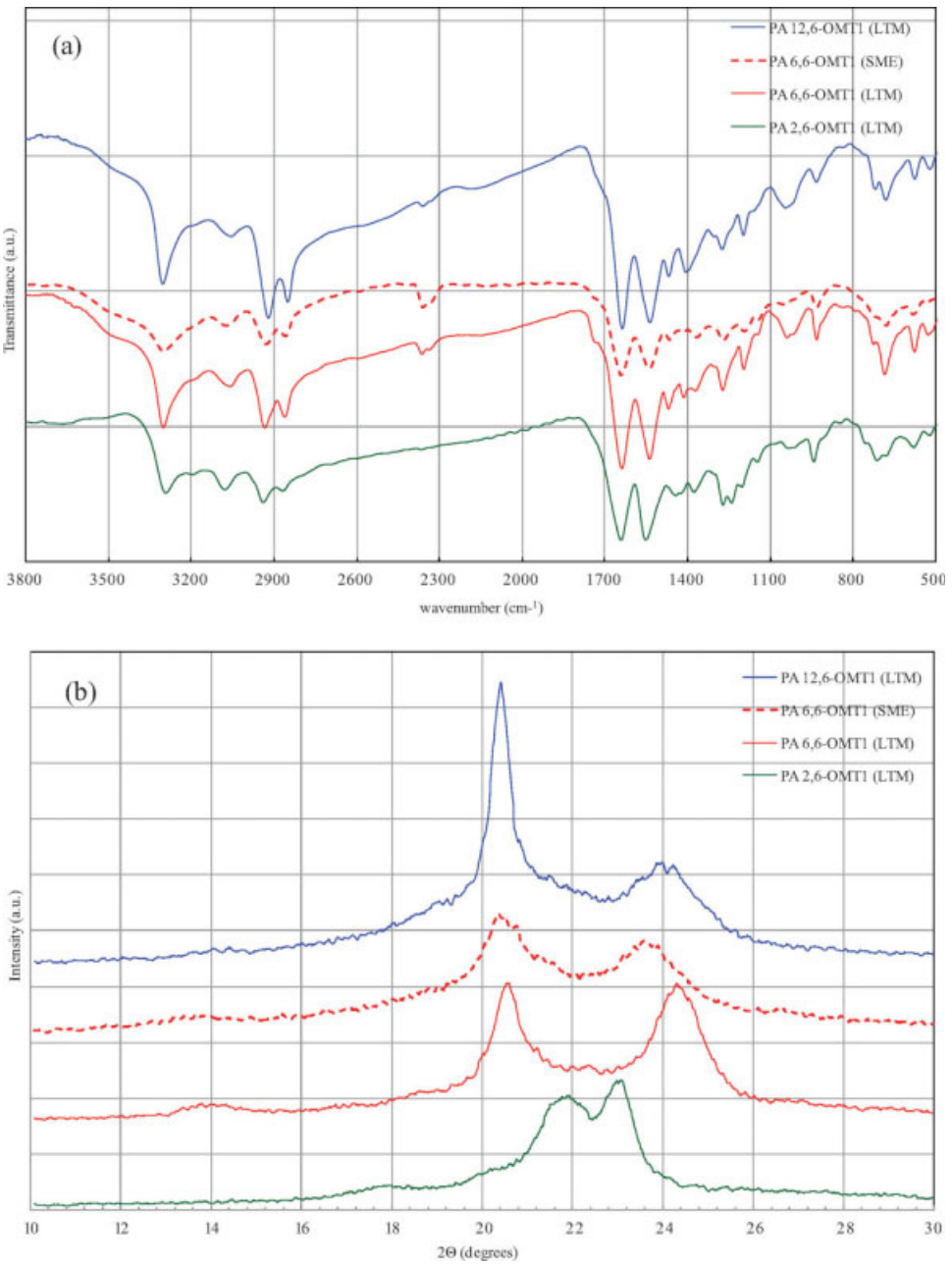

Figure 1 Indicative (a) FTIR and (b) XRD spectra of PA *n*,6–clay grades obtained by low-temperature melt polycondensation (LTM) and solution-melt polycondensation followed by extrusion (SME) process. [Color figure can be viewed in the online issue, which is available at www.interscience.wiley.com.]

same *d*-spacing value (d = 13.6 Å at $2\Theta = 6.6^\circ$) in all grades and, respectively, a remarkable decrease of clay interlayer spacing in all organoclay cases, except for the unmodified clay, where intercalation occurs, but at the same *d*-spacing value of 13.6 Å at $2\Theta = 6.6^\circ$ (Fig. 3). Furthermore, it is noteworthy that when the starting material is 6,6–OMT1/CP, the deriving polyamide yields the same XRD spectrum as in the case of its monomer [Fig. 2 vs. 3(a)], proving that the structural modification induced during coprecipitation of the monomer, that is, sheet collapse, was irreversible.

Similar residual peaks indicating flocculated clay structures have been already reported in the literature concerning *in situ* polymerizations of polyamide–organoclay in the case of diamine–diacid reactants. Nevertheless, they either have not been further evaluated[19] or they have been attributed to thermal degradation of organoclay,[17] which is anticipated—especially in melt intercalation processes—due to elevated temperature profiles applied in polyamides cases. However, in our experimental cases, the latter is rather avoided because of benign temperature–time profile. Even more, we also

TABLE II
Characterization of PA *n*,6–OMT1 Grades Prepared

	Thermal analysis			Solution viscometry
	T_m (°C)	ΔH_f (cal g^{-1})	x_c %	[η] (dL g^{-1})
Low-temperature melt polycondensation				
PA 2,6–OMT1 (LTM)	324.21 ± 0.13	24.44 ± 0.57	48.4 ± 1.1	0.58 ± 0.08
PA 6,6–MT (LTM)	265.42 ± 1.48	15.69 ± 1.22	31.1 ± 2.4	0.50 ± 0.02
PA 6,6–OMT1(LTM)	263.82 ± 0.66	10.96 ± 0.09	21.7 ± 0.1	0.58 ± 0.02
PA 6,6–OMT1/CP(LTM)	264.77 ± 0.98	11.13 ± 1.12	22.1 ± 2.2	0.56 ± 0.01
PA 6,6–OMT2(LTM)	263.15 ± 0.25	11.96 ± 0.39	23.7 ± 0.8	0.53 ± 0.03
PA 12,6–OMT1 (LTM)	236.86 ± 0.45	9.39 ± 0.68	18.6 ± 1.3	0.62 ± 0.07
Solution-melt polycondensation and subsequent extrusion				
PA 6,6–OMT1(SME)	261.07 ± 2.41	8.84 ± 0.37	17.5 ± 0.7	1.02 ± 0.05
PA 6,6–OMT1/CP(SME)	260.27 ± 1.49	8.59 ± 0.46	17.0 ± 0.9	1.60 ± 0.07

experimentally confirmed this by performing heat treatments of the organoclays under similar conditions applied in the polymerization processes. The derived XRD spectra are presented in Figure 3 for comparison reasons, where it is evidenced that during the specific experimental conditions there is no collapse of the organoclay sheets due to surfactant degradation, as no shift of the d_{001} peak to higher angles was observed, apart from a decrease of peak intensity due to some anticipated loss of crystallinity.[37]

Turning to the effect of the polyamide type (PA *n*,6-based grades) on clay dispersion, the XRD spectra [Fig. 4(a)] showed that for the shorter diamine ETD flocculation of the silicate occurred, corresponding to smaller *d*-spacing (13.3 Å) than in HMD case (13.6 Å) (Table III). On the other hand, DMD led to intercalation of the silicate by the polyamide, as indicated by the increased interlayer spacing after polymerization (21.0 Å), compared to initial silicate *d*-spacing (18.2 Å).

PA 6,6 nanocomposites via solution-melt polycondensation process and subsequent extrusion

In this section, we focused on PA 6,6–clay nanocomposite case and applied a solution-melt polycondensation process similar to the predominant industrial process for PA 6,6 production, including a final step of twin-screw extrusion.[24] The monomer grades submitted to this process were 6,6–OMT1 dry blend salt and 66–OMT1 coprecipitate salt, and the polymerized grades are presented in Table I. Polyamide formation was again verified through the FTIR spectra

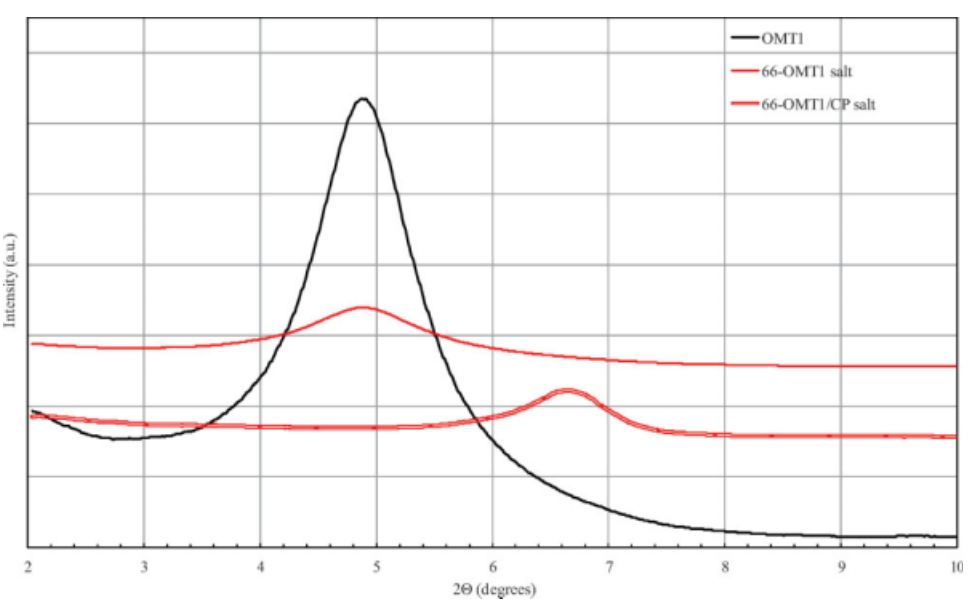

Figure 2 XRD spectra of PA 6,6–clay monomers derived from coprecipitation (6,6–OMT1/CP) and dry blending (6,6–OMT1). For comparative reasons, the nanofiller spectrum is presented. [Color figure can be viewed in the online issue, which is available at www.interscience.wiley.com.]

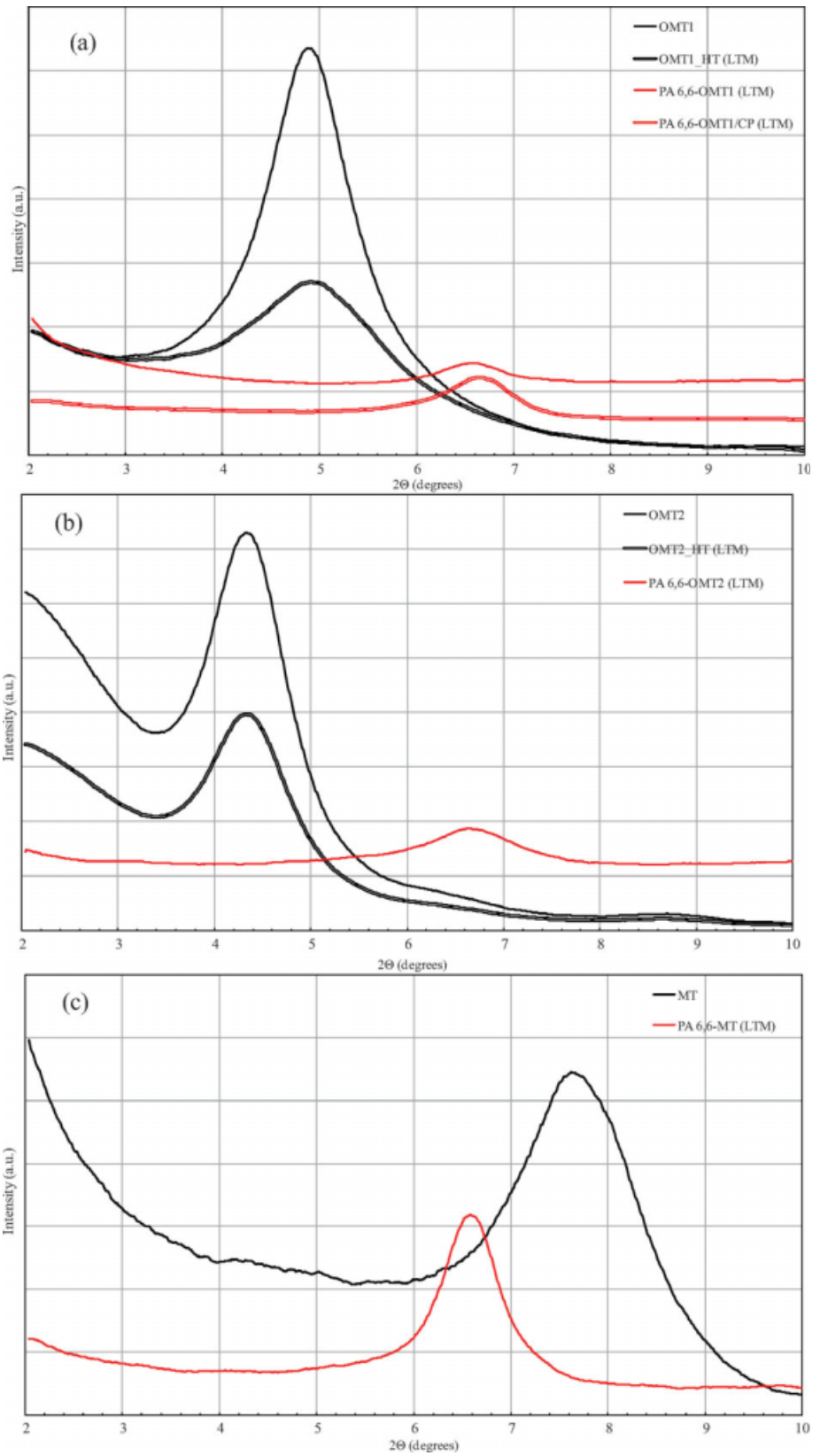

Figure 3 XRD spectra of PA 6,6–clay grades (2.5% w/w) obtained by low-temperature melt polycondensation (LTM) process, (a) PA 6,6–OMT1(LTM), PA 6,6–OMT1/CP(LTM), (b) PA 6,6–OMT2(LTM), and (c) PA 6,6–MT(LTM). For comparative reasons, the nanofillers and derived heat-treated spectra are presented. [Color figure can be viewed in the online issue, which is available at www.interscience.wiley.com.]

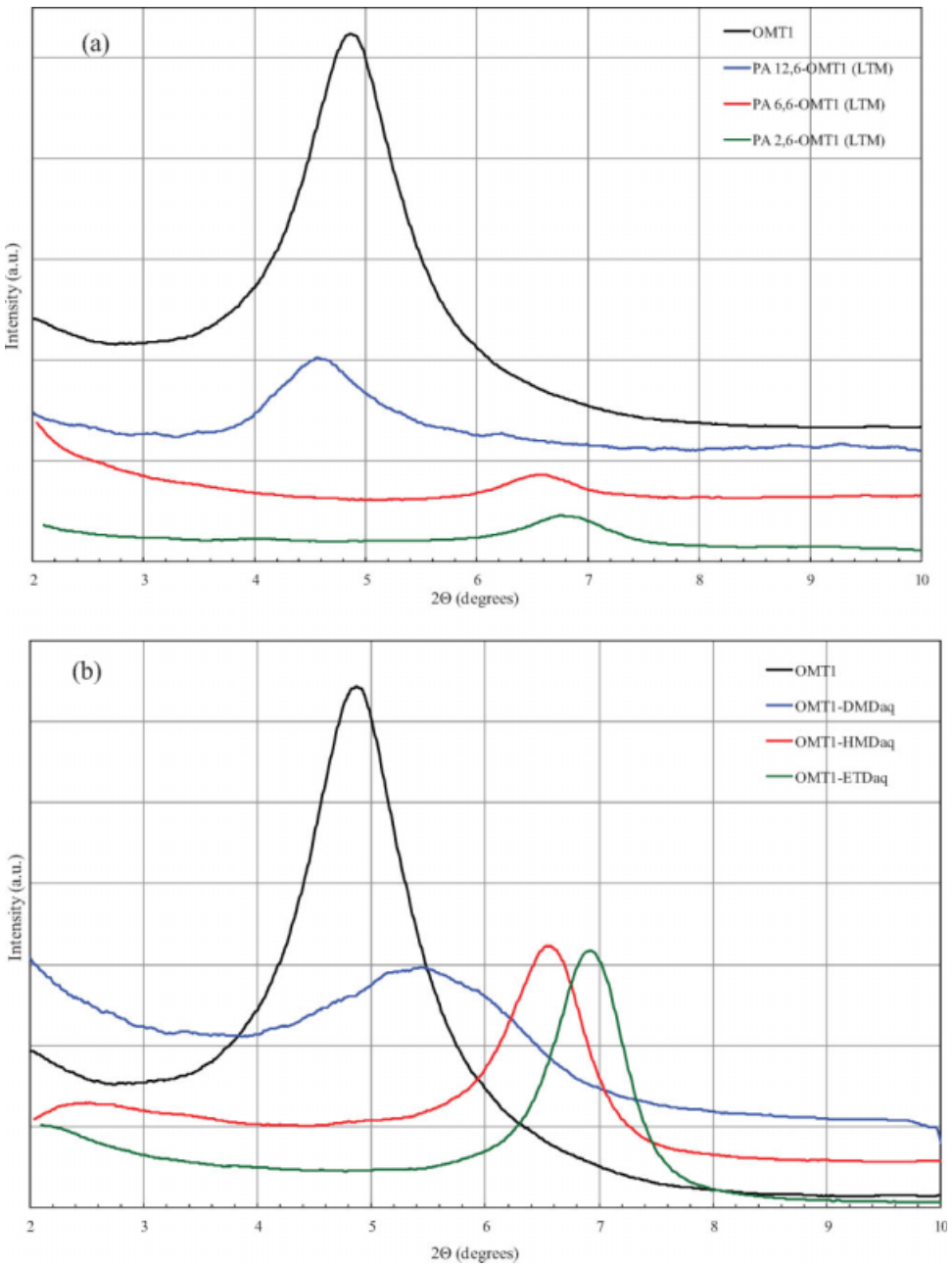

Figure 4 XRD spectra of (a) PA *n*,6–OMT1 grades (2.5% w/w) obtained by low-temperature melt polycondensation (LTM) process and (b) OMT1–ETD_{aq}, OMT1–HMD_{aq}, and OMT1–DMD_{aq}. For comparative reasons, the nanofiller spectrum is presented. [Color figure can be viewed in the online issue, which is available at www.interscience.wiley.com.]

obtained and indicatively presented for PA 6,6–OMT1(SME) [Fig. 1(a)], as both grades gave absorptions at 3300 cm^{-1} (amide I, hydrogen-bonded NH vibration) and 1640 cm^{-1} (amide I, C=O stretch).[24] The obtained WAXD profiles as indicatively presented for PA 6,6–OMT1(SME) [Fig. 1(b)] indicated a typical triclinic lattice (α-form) with the chains in fully extended zigzag conformation,[35] as previously discussed. The melting points and crystallinities were determined and found slightly lower than respective PA 6,6–OMT1 via LTM process, due to faster crystallization conditions after extrusion (Table II). The intrinsic viscosity values indicated the formation of average molecular weight polyamides (Table II), being higher than LTM process due to more intense reaction conditions and subsequent extrusion. Finally, the nanofiller incorporation was verified by ashing, and the content was determined to be 2.39% w/w for PA 6,6–OMT1(SME) and 2.76% w/w for PA 6,6–OMT1/CP(SME).

Turning to the nanocomposite structure obtained, based on the XRD spectra of both grades (Fig. 5), the

TABLE III
XRD Features of Prepared PA *n*,6–Clay Grades and Organoclay OMT1 After Treatment with Diamine Aqueous Solutions

	Polyamide grades		
	Clay *d*-spacing (Å)	PA grade *d*-spacing (Å)	Δd (Å)
Low-temperature melt polycondensation			
PA 2,6–OMT1(LTM)	18.2	13.3	−4.9
PA 6,6–MT (LTM)	12.9	13.6	+0.7
PA 6,6–OMT1 (LTM)	18.2	13.6	−4.6
PA6,6–OMT1/CP(LTM)	18.2	13.6	−4.6
PA 6,6–OMT2 (LTM)	20.0	13.6	−6.4
PA 12,6–OMT1 (LTM)	18.2	21.0	+2.8
Solution-melt polycondensation and subsequent extrusion			
PA 6,6–OMT1 (SM) and/or (SME)	18.2	13.6	−4.6
PA 6,6–OMT1/CP (SM) and/or (SME)	18.2	13.6	−4.6
	Organoclay treatment with diamine aqueous solutions		
	Clay *d*-spacing prior treatment (Å)	Clay *d*-spacing posttreatment (Å)	Δd (Å)
OMT1–ETDaq	18.2	13.3	−4.9
OMT1–HMDaq	18.2	13.6	−4.6
OMT1–DMDaq	18.2	16.2	−2.0

same picture as in LTM polycondensation is encountered. The residual peak at $2\Theta = 6.6^\circ$ ($d = 13.6$ Å) is persistent, regardless of the polymerization process applied and/or the monomer nature (dry blend or coprecipitate) (Table III). In other words, the diminishment of the silicate interlayer from 18.2 to 13.6 Å seems to be insensitive to polymerization scaling up, where more intensive stirring conditions should enhance silicate dispersion. Even more, Figure 5 reveals that a final process step of twin-screw extrusion did not improve the latter, showing the irreversible character of flocculation under the specific experimental conditions, polyamide matrix, and organoclay combination.

Organoclay–PA *n*,6 interaction mechanism

Based on the above observations, an intrinsic interaction between the PA salt constituent diamine and the clay/organoclay is assumed, as there is a lack of exfoliation in all experimental cases described, combined with dependence of the achieved silicate interlayer distance on the PA salt diamine length (*n*). To confirm the diamine–surfactant interaction, we used an aqueous solution technique resembling the typical organophilization routine, in which different diamines were left to interact with a specific organoclay; as it can be clearly observed in the XRD spectra of the resulted products [Fig. 4(b)], the silicate interlayer spacing changes in respect to the diamine length, verifying the previously quoted results of the PA *n*,6 grades (Table III).

The two species involved in the indicated interaction, that is, PA salt diamine and organoclay surfactant, are competitive ions and can participate in ion exchange reactions, especially when a suitable environment of sufficient ionic mobility is provided. Pertinent ion exchange reactions usually occur in solutions, but have also been reported in solid state,[38] indicating the spontaneity of such, when reactivity and/or thermodynamic conditions are fulfilled. The described ion exchange reaction is driven by the chemical resemblance of the involved moieties and defined by their size and extent of functionality. More specifically, the bisfunctionality and small size of salt diamine cations favor the replacement of the monofunctional, large surfactant ones, as the more bulky the cation, the lower its degree of stabilization; as a consequence, protonated HMD replaces the organoclay surfactant or even the sodium cations in all PA 6,6-based grades, resulting in a hexamethylenediammonium-modified clay with sheets ionically bonded from both sides (Fig. 6) and characterized by a *d*-spacing value locked at 13.6 Å.

Indeed, in short diamines like HMD and ETD, the described ion exchange leads to an irreversible diminishment of the *d*-spacing due to strong electrostatic interactions between the counter ions of the diamines and the clay layers, thus inhibiting any significant intercalation, even if twin-screw extrusion is attempted as a final step in PA 6,6 matrix (Fig. 5). On the other hand, when a longer chain diamine (DMD) is used, the achieved *d*-spacing of

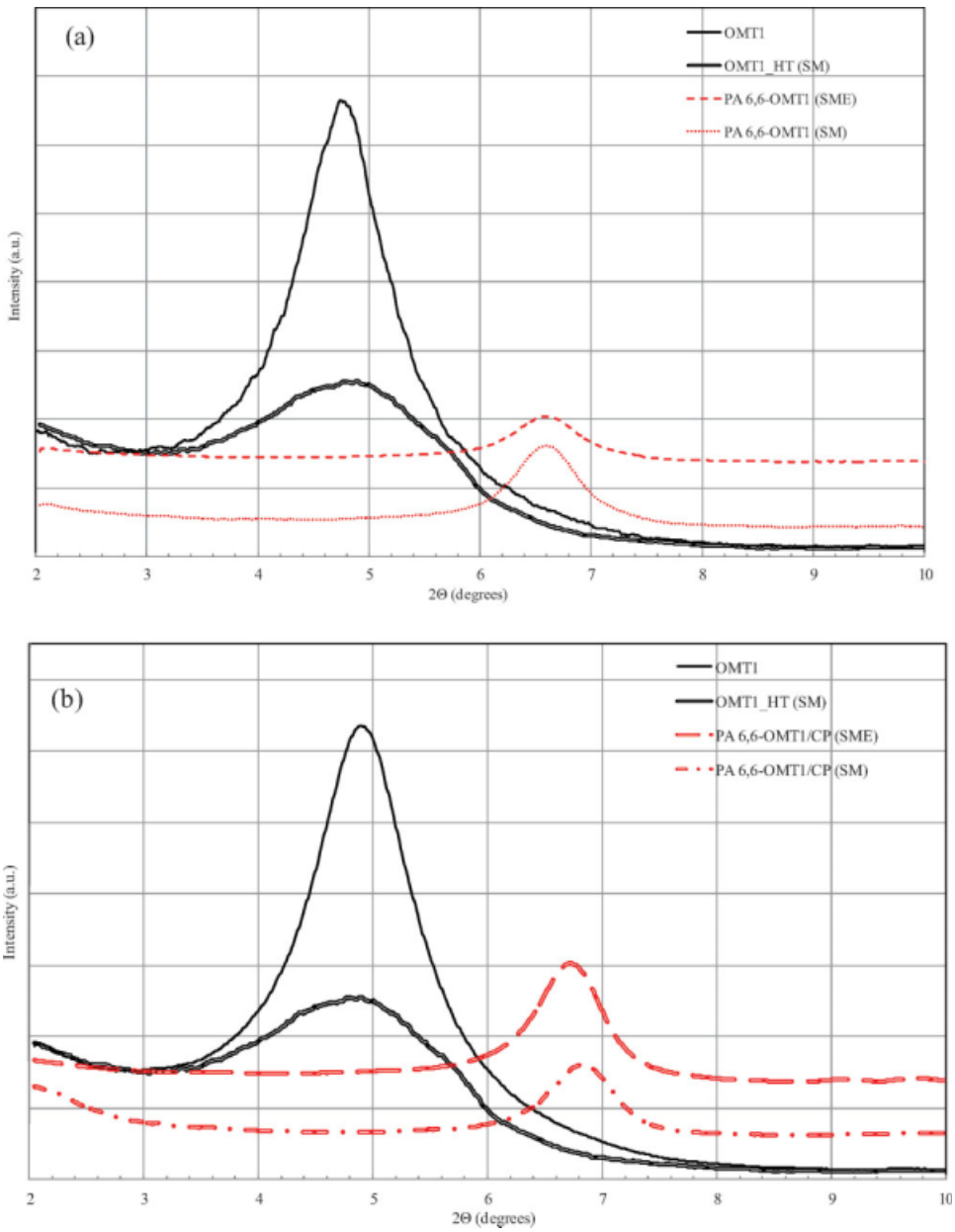

Figure 5 XRD spectra of (a) PA 6,6–OMT1 and (b) PA 6,6–OMT1/CP grades (2.5% w/w) obtained by solution-melt polycondensation (SM) process and relevant extrudates (SME). For comparative reasons, the nanofiller and derived heat-treated spectrum are presented. [Color figure can be viewed in the online issue, which is available at www.interscience.wiley.com.]

dodecamethylenediammonium-modified clay is high enough to accommodate the growing, during polymerization, PA 12,6 chains. The latter observation derives from the increased *d*-spacing value (21.0 Å) obtained in the PA 12,6–OMT1(LTM) case versus OMT1–DMD_{aq} (16.5 Å) [Fig. 4(a) vs. Fig. 4(b)]: the interlayer spacing achieved in the former case corresponds to intercalated PA 12,6 chains, whereas in the latter corresponds to DMD configuration between the silicate sheets, in contrast with the OMT1–ETD_{aq} and OMT1–HMD_{aq} grades, where *d*-spacings seem locked in the range of 13.3–13.6 Å (Table III).

CONCLUSIONS

This article aimed at the synthesis of PA *n*,6–clay nanocomposites, namely PA 2,6, PA 6,6, and PA 12,6, via *in situ* polycondensation. For this purpose, two different polymerization routes were considered; a low-temperature melt polycondensation and

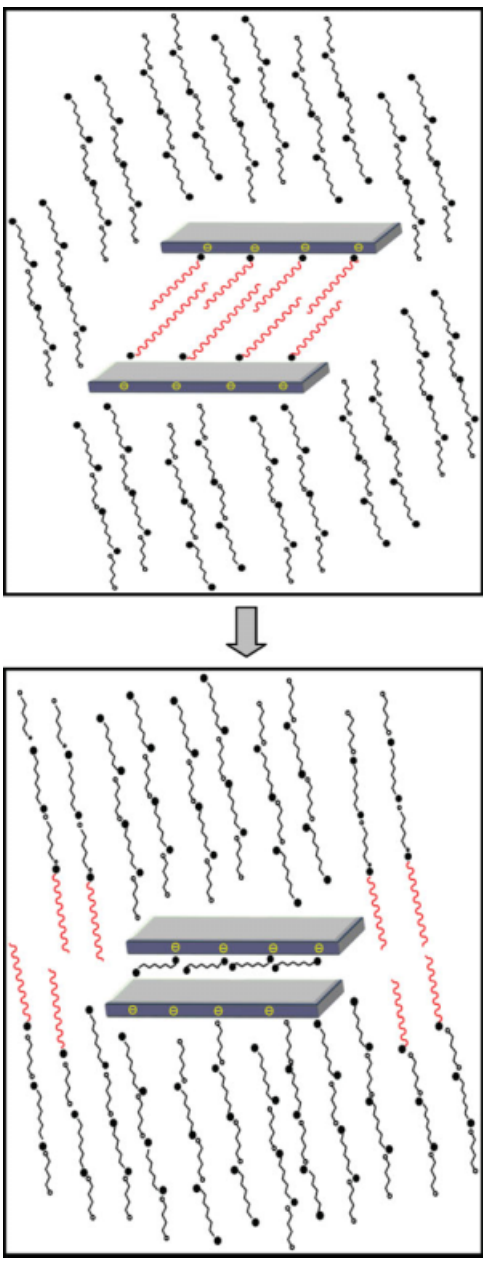

Figure 6 Indicative schematic depiction of cation exchange mechanism between the surfactant of organoclay and PA 6,6 salt diamine. ● = NH_3^+, ○ = COO^-, ∿∿∿ = polyamide salt methylene groups, ∿∿∿∿∿ = surfactant tallow. [Color figure can be viewed in the online issue, which is available at www.interscience.wiley.com.]

a solution-melt one followed by extrusion. Both techniques resulted in polyamides with adequate properties to assess the nanocomposite formation potential. The obtained grades exhibited a collapse of silicate interlayer spacing despite the different polymerization attributes, such as temperature profile, aqueous environment, and shear existence, which proved irreversible even when melt intercalation through extrusion was attempted as a final step. Furthermore, dependence of the resulting PA *n*,6–clay structures on the diamine constituent of PA monomer was found. The research findings revealed an intrinsic interaction between the salt diamine and the surfactant cations; a pertinent mechanism was proposed, according to which an ion exchange occurs between these two competitive moieties, due to the bisfunctionality and small size of salt diamine. This silicate interlayer collapse proved to be irreversible in short diamine salts, like PA 2,6 and 6,6 salts, as the small interlayer spacing was insufficient to accommodate the growing polyamide chains. On the contrary, in the case of longer diamine salts, like PA 12,6 salt, the resulting interlayer spacing was adequately high to allow for the polyamide to intercalate and expand the silicate sheets, yielding intercalated nanocomposite structure.

The authors thank Süd Chemie AG and Rockwood Additives Ltd. for providing the nanofillers used. Prof. A. Tsolomytis contribution on organic chemistry issues is deeply appreciated.

References

1. Pavlidou, S.; Papaspyrides, C. D. Prog Polym Sci 2008, 33, 1119.
2. Ray, S.; Okamoto, M. Prog Polym Sci 2003, 28, 1539.
3. Lagaly, G. Clay Miner 1981, 16, 1.
4. Greenwell, C.; Harvey, M.; Boulet, P.; Bowden, A.; Coveney, P.; Whiting, A. Macromolecules 2005, 38, 6181.
5. Yoshida, O.; Okamoto, M. Macromol Rapid Commun 2006, 27, 751.
6. Cho, J. W.; Paul, D. R. Polymer 2001, 42, 1083.
7. Dennis, H. R.; Hunter, D. L.; Chang, D.; Kim, S.; White, J. L.; Cho, J. W.; Paul, D. R. Polymer 2001, 42, 9513.
8. Fornes, T. D.; Yoon, P. J.; Kesskula, H.; Paul, D. R. Polymer 2001, 42, 9929.
9. Chavarria, F.; Paul, D. R. Polymer 2004, 45, 8501.
10. Liu, X.; Wu, Q. Macromol Mater Eng 2002, 287, 180.
11. Zhu, C. S.; Kang, X.; He, S. Q.; Wang, L. Y.; Lu, L. Y. Chin J Polym Sci 2002, 20, 551.
12. Kang, X.; He, S.; Zhu, C.; Lü, W. L.; Guo, J. J Appl Polym Sci 2005, 95, 756.
13. Mehrabzadeh, M.; Kamal, M. R. Polym Eng Sci 2004, 44, 1152.
14. Xie, W.; Gao, Z.; Pan, W.; Hunter, D.; Singh, A.; Vaia, R. Chem Mater 2001, 13, 2979.
15. Fornes, T. D.; Yoon, P. J.; Paul, D. R. Polymer 2003, 44, 7545.
16. Yano, K.; Usuki, A.; Okada, A.; Kurauchi, T.; Kamigaito, O. J Polym Sci Part A: Polym Chem 1993, 31, 2493.
17. Song, L.; Hu, Y.; He, Q.; You, F. Colloid Polym Sci 2007, 286, 721.
18. Goettler, L.; Joardar, S. WO Pat. 0,009,571 (2002).
19. Wu, Z.; Zhou, C.; Qi, R.; Zhang, H. J Appl Polym Sci 2002, 83, 2403.
20. Kalkan, Z. S.; Goettler, L. A. SPE ANTEC 2006, 1, 538.
21. Tynan, D. G.; Papaspyrides, C. D.; Bletsos, I. V. U.S. Pat. 5,941,634 (1999).
22. Papaspyrides, C.; Vouyiouka, S.; Bletsos, I. J Appl Polym Sci 2004, 92, 301.
23. Papaspyrides, C.; Vouyiouka, S. Solid State Polymerization; Wiley: New Jersey, 2009.

24. Nelson, W. Nylon Plastics Technology; Butterworths: London, 1976; p 214.
25. Hiemenz, P. Polymer Chemistry: The Basic Concepts; Marcel Dekker: New York, 1984; p 304.
26. Papaspyrides, C. D.; Kampouris, E. M. Polymer 1986, 27, 413.
27. Papaspyrides, C. D.; Kampouris, E. M. Polymer 1986, 27, 1433.
28. Papaspyrides, C. D. Polymer 1988, 29, 114.
29. Papaspyrides, C. D. Polym Int 1992, 29, 293.
30. Benjamin, S. M. U.S. Pat. 6,117,550 (2000).
31. Vouyiouka, S.; Koumantarakis, G.; Papaspyrides, C. J Appl Polym Sci 2007, 104, 1609.
32. Boussia, A. C.; Vouyiouka, S. N.; Papaspyrides, C. D. Presented at the 9th European Symposium on Polymer Blends; Conference Proceedings, Palermo, Italy, 2007; p 97.
33. Solomon, O.; Ciuta, I. J Appl Polym Sci 1962, 6, 683.
34. Vasanthan, N.; Murthy, S.; Bray, G. Macromolecules 1998, 31, 8433.
35. Murthy, S. J Polym Sci Part B: Polym Phys 2006, 44, 1763.
36. Korshak, V.; Frunze, T. Synthetic Hetero–Chain Polyamides; IPST: Jerusalem, 1964; p 344.
37. Kiricsi, I.; Palinko, I.; Tasi, G.; Hannus, I. Mol Cryst Liq Cryst 1994, 244, 149.
38. Ogawa, M.; Hagiwara, A.; Handa, T.; Kato, C.; Kuroda, K. J Porous Mater 1995, 1, 85.